J. Anat. (1996) 188, pp. 1–15, with 8 figures Printed in Great Britain

Review

'If you assume, you can make an ass out of u and me': a decade of the disector for stereological counting of particles in 3D space

T. M. MAYHEW[1] AND H. J. G. GUNDERSEN[2]

[1] *Department of Human Morphology, University of Nottingham, UK, and* [2] *Stereological Research Laboratory, Aarhus University, Aarhus, Denmark*

(*Accepted 30 May 1995*)

ABSTRACT

The year 1984 was a watershed in stereology. It saw the introduction of highly efficient and unbiased design-based methods for counting the number of arbitrary objects in 3-dimensional (3D) space using 2D sectional images. The only requirement is that the objects be unambiguously identifiable on parallel sections or successive focal planes. The move away from the 'assumption-based' and 'model-based' methods applied previously has been a major scientific advance. It has led to the resolution of several problems in different biomedical areas. The basic principle which makes possible 3D counting from sections is the disector. Here, we review the disector principle and consider its impact on the counting and sizing of biological particles. From now on, there can be no excuse for applying the biased counting methods of yesteryear. Their continued use, despite the availability of unbiased alternatives, should be seen as paying homage to History rather than advancing Science.

Key words: Particle counting; stereology; disector

INTRODUCTION

During the past decade, stereology has developed to the extent that it is now the technique of first choice whenever 3D structural quantities need to be extrapolated from planar measurements performed on 2D slice images. Before 1984, stereological methods for estimating particle number and size relied on assumptions about particle shape, size and orientation (e.g. Weibel, 1979). Unfortunately, these 'model-based' and 'assumption-dependent' approaches are in general not unbiased. In fact, they are only valid in special cases, i.e. those in which the model or assumptions *faithfully* mimic reality.

The dangers of using model or assumption-based approaches are twofold: (1) the ideal and reality seldom coincide and (2) the resulting bias is usually unknown because the underlying assumptions go untested. Consequently, the impact of bias on the accuracy of estimation and the validity of biological conclusions is also unknown. The dangers are expressed succinctly in the pun-phrase of the title of this review: 'If you *ass-u-me*... you can make an *ass* out of *u* and *me*!' (Harris, 1991).

Assumption-free methods offer an important additional benefit: they are highly efficient. In other words, they offer greater precision per unit cost (Gundersen & Jensen, 1987; Gundersen et al. 1988*a*, *b*; Cruz-Orive & Weibel, 1990; Mayhew, 1991*a*, 1992). Both validity and efficiency are determined by design-based random sampling, i.e. by generating random encounters between the specimen and test probes. An extremely efficient way of drawing random samples from specimens is systematic sampling (Gundersen & Jensen, 1987). This can be applied at all levels of the sampling process, e.g. cut an organ into uniform random slices, select tissue blocks from the slices in a systematic manner, cut parallel sections

Correspondence to Professor T. M. Mayhew, Department of Human Morphology, Queen's Medical Centre, University of Nottingham, Nottingham NG7 2UH, UK.

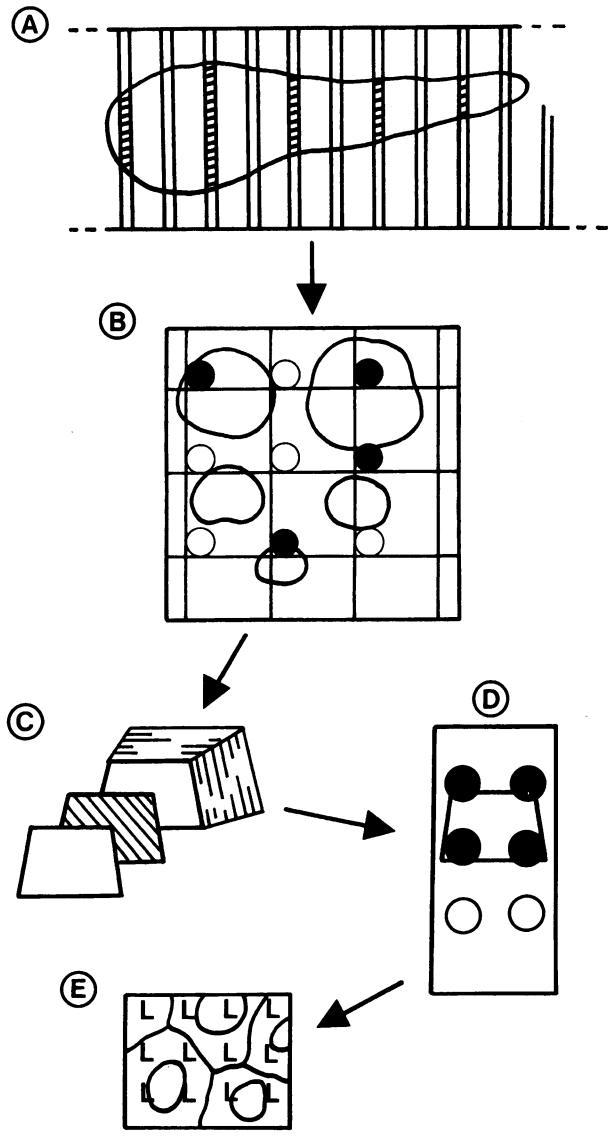

Fig. 1. An illustration of a systematic random (SR) sampling scheme. At *stage A* an organ is cut into uniform random slices so that all positions along the organ have an equal chance of being cut. A systematic subset of these slices (hatched) is taken for further sampling at *stage B* in which the subset is shown covered by a randomly positioned square lattice. An SR sample of tissue plugs is taken from circular holes drilled in the lattice and those overlying tissue slices (black circles) provide samples which are block-embedded for microtome sectioning. At *stage C* sections are cut from blocks. A sampled section (hatched) is placed on a glass microslide from which an SR sample of fields containing tissue (black circles) is obtained using the x and y axes of a microscope stage (*stage D*). Finally, at *stage E* a regular array of test points (represented by the inner corner point of each L) is superimposed on sections to obtain an SR sample of chance encounters with tissue components visible on those sections. Only by random sampling at *each* stage is a good (unbiased) sample obtained. If, at any stage, the chain is broken by nonrandom sampling, this will lead to a bad (biased) sample.

from tissue blocks at a set distance and, finally, place a regular pattern of test probes on those sections (Fig. 1).

This review focuses attention on unbiased and efficient counting of arbitrary particles using systematic sections. In this context, a 'particle' might be a corpuscle (e.g. a nucleus or cell), an associated feature (e.g. the pore or mouth of a gland or an incompletely interiorised endosome), a space (e.g. a void, cavity or perforation) or a structural element (e.g. a trabecula or capillary unit). Moreover, these features may be discrete or connected in complicated ways (e.g. capillary units forming a capillary bed).

To count and size particles, the test probes required are volumes, points and lines. The test volume probes might comprise systematic sets of pairs of section planes separated by a known distance. The test points and test lines might form a regular array (a test grid or lattice) on a transparent overlay or an eyepiece graticule. Such grids are superimposed on random section planes or on microscopical fields randomly sampled within those sections. For stereological estimation of particle number, section planes must be used and these must be randomly located. Estimating size may require that section planes are also randomly oriented.

BRIEF HISTORICAL PERSPECTIVE

There have been many different approaches to estimating particle number. They include maceration, biochemistry and sectional morphometry. Maceration has been used to isolate and count renal glomeruli and pancreatic islets of Langerhans. In the case of glomeruli, acid maceration is time-consuming and may damage some of the particles (for a review, see Bendtsen & Nyengaard, 1989). Biochemical estimates of DNA have several disadvantages including inability to distinguish (1) nuclei belonging to different cellular (or syncytial) compartments and (2) many diploid from few polyploid nuclei. Cells and syncytia may also have no nucleus or more than one nucleus so that counting nuclei may not be a valid way of estimating 'cell' number. Combining DNA content with protein content has been used to estimate cell size, expressed as protein/DNA ratio. This approach does not have general validity. It works only for homogeneous tissues which are exclusively cellular and cannot be applied to syncytia or to tissues which comprise mixtures of cells and extracellular space/matrix. In the latter case, a protein/DNA ratio will not distinguish hypertrophic from interstitial growth. Despite these deficiencies, DNA and protein contents have been used to monitor the growth and development of organs, e.g. placenta and skeletal muscle (for some recent references, see Simpson et al. 1992;

Wigmore et al. 1992; Mayhew & Simpson, 1994; Mayhew et al. 1994*b*).

The stereological approach is better. First, identify particles by appropriate criteria (where necessary, using techniques which aid identification, such as immunochemistry or enzyme histochemistry) and then count them. Often, we are forced to undertake such counts using histological or other sections. In the past, counting in 3D from sectional images of particles was based entirely on assumptions. For example, cells and their nuclei have been modelled as spheres, synapses as circular discs and mitochondria as circular cylinders.

Although often confounded by inadequacies of sampling as well, these model-based methods were, at least before 1980 (Cruz-Orive, 1980), the best available at the time. They recognised that the probability of particles being cut by single sections depends on several factors, including section thickness, section angle, particle size and particle shape. These are important considerations because a 2D set of cell profiles does not provide a generally valid indication of the number of 3D cells which, on sectioning, gave rise to them. Thus large cells (e.g. megakaryocytes, macroneurons) have more chance of being cut than small cells (e.g. lymphocytes, microneurons). Similarly, uninucleate cells generate sectional images which comprise more cell profiles than nuclear profiles because cells are bigger than their nuclei. Furthermore, fusiform cells (e.g. smooth muscle cells) have more chance of being cut by transverse than by longitudinal sections. Finally, an irregular particle (e.g. the nucleus of a polymorphonuclear leucocyte) can be cut in several places by the same section plane. Without some additional information (such as knowing that each polymorph has one nucleus), this phenomenon may make it difficult to decide whether or not the several profiles appearing on the section plane belong to just one particle.

Using single sections (areal probes) introduces errors governed by size, shape and spatial orientation (see Fig. 2). In fact, single sections sample particles not only on the basis of how many there are but also with a probability determined by particle size (height) in the direction normal to the section plane. Therefore, single sections provide a *biased* selection of particle profiles, i.e. they preferentially select particles of greater height. Fortunately, we can avoid these problems and obtain unbiased estimates of particle number by sampling them with volume probes (Gundersen, 1986; Cruz-Orive, 1987*a*).

A significant technical advance, i.e. independence of particle shape, size distribution or orientation, was made by Cruz-Orive (1980). He suggested using a volume probe which consisted of a stack of serial sections cut with a random start position but at an arbitrary orientation. This pioneering approach has been succeeded by more efficient alternatives based on the disector (Sterio, 1984; Gundersen, 1986) which relies on pairs of parallel sections.

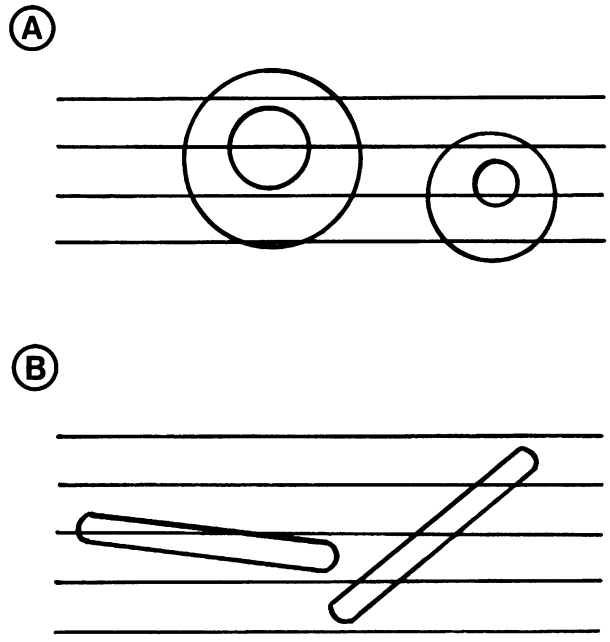

Fig. 2. The effects of orientation, size and shape on the probability of sectioning. (A) A set of 4 sections is cut through 2 spherical cells, each cell harbouring a single spherical nucleus. Although there is 1 large cell and 1 small cell, note that the larger cell produces more profiles (these will appear as circles) when sectioned. In this example, there would be 7 cell profiles but only 2 nuclear profiles. So our estimate of cell number would depend also on whether we adopted the nucleus or the cell as the counting unit. (B) A rod-shaped particle has a greater probability of being sectioned when its long axis is orthogonal to the section plane and a lower probability when it is parallel to that plane. These observations illustrate the point that isolated sections cannot, in general, provide valid data on particle number. Because number is zero-dimensional, a 3D probe is required to count particles in 3D space.

ASSUMPTION-FREE COUNTING—THE DISECTOR

The basic principle

With the disector (Fig. 3), particles are counted with an unbiased 3D counting rule using pairs of parallel planes separated by a known distance, d. The only requirement about particle shape is that it must be possible to identify all particle profiles on sections which belong to the same parent particle. Particles which fail to meet this basic condition (Cruz-Orive, 1980; Gundersen, 1986) cannot be counted by stereology.

Each disector pair should be randomly located within the specimen. The rule is to count only those

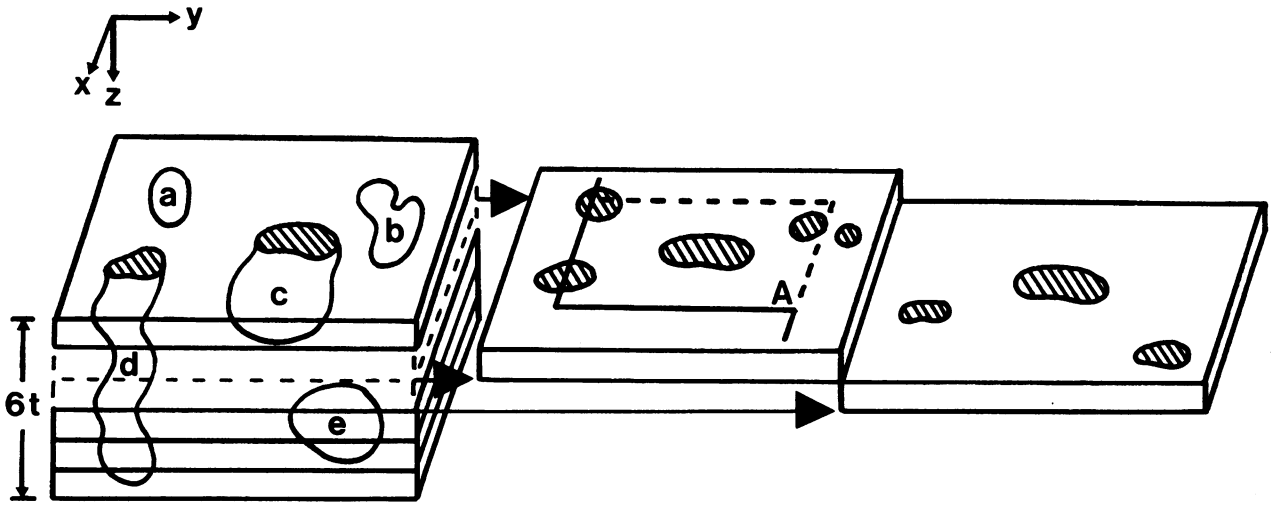

Fig. 3. The disector principle. The diagram shows a block of tissue containing 5 identified particles (a–e) and cut serially into parallel sections. A pair of adjacent sections (a physical disector) is drawn from the stack and their upper faces are shown. Note that these are separated by a distance equal to the thickness (t) of one section. The uppermost ('reference') section bears an unbiased counting frame of area A, whilst the lower ('look-up') section does not. The volume of the disector is equal to $A \times t$. Note that only particles a–d appear on the reference section. However, particles a, c and d are not eligible for counting for the following reasons: particle a because it touches the forbidden line of the counting frame, particle c because it also appears on the look-up section and particle d for both reasons. Only particle b is counted: although it is non-convex and appears as 2 profiles on the reference section, it does not touch the forbidden lines (or their extensions) or appear on the look-up section. It is a condition of unbiased counting that we must know that both profiles belong to the same parent particle. In this example, $Q^- = 1$ and $N_v = 1/(A \times t)$.

particles which appear in an unbiased counting frame on one plane (the *reference* plane) but not on its partner (the *look-up* plane). Several unbiased counting rules are available for deciding whether or not particle profiles can be regarded as being included in the counting frame on the reference plane (Gundersen, 1977; Miles, 1978; Jensen & Sundberg, 1986). The number of particles meeting the counting criteria, by convention given the symbol Q^-, is contained within the volume of the disector. This volume is equal to the area of the counting frame, A, multiplied by the distance between the planes (Fig. 3). Therefore, the numerical density of particles in the reference volume (N/V) is estimated by

$$\text{est}\, N/V = \Sigma Q^-/(\Sigma A \times d).$$

If the specimen has been sampled systematically by multiple disectors, N/V is calculated after summing A and Q^- over all disectors. An efficient way of estimating ΣA for a set of disectors is via

$$\text{est}\, \Sigma A = \Sigma P \times a$$

where ΣP is the total number of test points which lie within the set of counting frames and a is a constant, i.e. the area associated with one test point.

Notice that the disector alone yields numerical density rather than number (N) itself. In consequence, estimates are sensitive to preparation artefacts such as fixation distortion (shrinkage or swelling). The disector is not affected by the sectioning artefacts of image over-projection and truncation provided that it is based on physical rather than optical sectioning (see below). However, its use does demand an accurate estimate of the plane separation, d. Fortunately, modifications of the use of the disector can circumvent the distortion artefacts and the need to know d (see below).

The orientation of the planes is not critical for achieving unbiased estimates of particle number with the disector but it may influence efficiency. It follows that convenient directions can be selected arbitrarily so as to improve efficiency. Moreover, the same pair of planes may be used in both forward (reference to look-up) and reverse (look-up to reference) directions and the average of these two counts can be taken. Clearly, different particles are selected in the two directions.

Practical implementation

A very efficient way of generating disectors is to track through successive focal planes in a thick slice of tissue. This is referred to as the *optical* disector. If this is not practicable, it is possible to cut physical sections (*physical* disectors) with some suitable cutting aid. With very densely packed particles (e.g. granule cell neurons in the cerebellum), the optical is preferable to the physical disector. Indeed, optical sectioning will

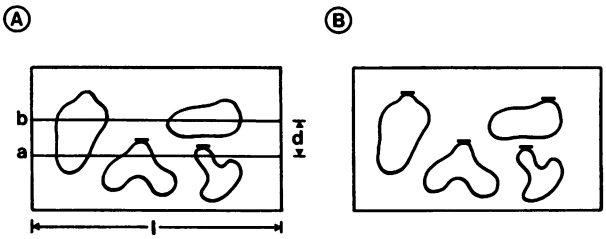

Fig. 4. An illustration, in 2D, of the physical and optical disector principles. (A) Four profiles are seen contained in a defined plane. The lines a and b, each of length l, are equivalent to the 'reference' and 'look-up' of a *physical* disector and are separated by a distance (d) which is smaller than profile height in the direction orthogonal to the lines. Two profiles are transected by line a but not line b and so are counted. We can imagine that both profiles have an associated point (e.g. the tangent to its uppermost pole) which is contained within the space lying between lines a and b. The 2 profiles counted lie in an area equivalent to $l \times d$. (B) We may imagine a line sweeping across the plane from its lower to upper edges. In so doing, we will count 4 such associated points. This is analogous to the *optical* disector in which a series of focal planes sweeps through a volume and encounters associated points of 3D particles.

probably supercede physical sectioning for histological studies. However, only physical disectors can be used with conventional transmission electron microscopy (TEM). The principles behind the two varieties of disector are illustrated simply in Figure 4.

Optical disectors. Parallel planes of focus will encounter particles for the first time only once and, therefore, all particles will have exactly the same probability of being selected and counted. This is the basis of the optical disector and, essentially, there are two main ways of generating optical sections. In both, the distance d (measured along the z-axis of the microscope) must be measured accurately, e.g. with a microcator (see Braendgaard et al. 1990, wherein the device measures to the nearest 0.5 μm). Vertical translations may be monitored conveniently by fitting an acoustic depth alarm to the fine focus control (Laroye & Taylor, 1992).

The first approach is *thin-focus* microscopy. For transmitted light microscopy, thick sections can be cut and focused at different focal planes (Gundersen, 1986). A particle is counted when it (or some part of it, such as its equator or its upper pole) first comes into focus within the counting frame. The use of high numerical aperture, oil-immersion objectives serves to ensure that movements in the z-direction represent true movements of the focal plane through the thick section. With glycol methacrylate as an embedding medium, optical sectioning in thick sections (25 μm or thicker) can be performed with minimal shrinkage distortion.

The second approach is *confocal* microscopy. If particles exhibit fluorescence or reflectance, they can be optically sectioned with a confocal microscope. Counting can then proceed with an unbiased 3D counting 'brick' (Howard et al. 1985).

Unlike the physical disector, the optical disector may produce biased estimates of numerical density if the 3D sampling probe extends to the bottom surface of the thick section. The bias is related to the 'lost cap' phenomenon (Gundersen, 1986) and can be avoided by restricting the sampling volume to the middle part of the section. For example, to a volume probe of height 15 μm at the centre of a 25 μm thick section. The same phenomenon may introduce bias into section thickness estimates, particularly if the section surfaces are highly irregular. For this reason, plastic sections are preferable to paraffin or frozen sections. The final sections should not be less than 25 μm thickness and objective lenses should be of high numerical aperture to ensure that the depth of focus is as small as possible. For a more comprehensive discussion of these problems, see Gundersen (1986) and West et al. (1991).

Physical disectors. Physical (mechanical) sections may be cut by knife, razor-blade or microtome. In this case, for reasons of efficiency, the sections should be separated by a distance d which is roughly a third to a quarter of particle size. Of course, d must never be greater than the size of the smallest particle in the direction normal to the section plane.

If d corresponds to section thickness t (or to some multiple of it), various options are available for determining section thickness and, thereby, section separation. They include Small's 'fold' method, microinterferometry, micrometry and section re-sectioning (see Goldstein & Hartmann-Goldstein, 1974; Weibel, 1979; Gundersen et al. 1983; Braendgaard & Gundersen, 1986; Bedi 1987; de Groot, 1988; Evans & Howard, 1989; Simpson et al. 1992).

Modifications of the disector

The need to estimate section separation can be avoided by adopting a suitable sampling design. Two possibilities exist: the first is comparable to that described originally for counting nerve fibre profiles in 2D on transected nerve trunks (and referred to in that context as the *ratio technique*; for references, see Mayhew, 1988) and the second is the *fractionator* (Gundersen, 1986).

The 'ratio technique'. Pakkenberg & Gundersen (1988) neatly avoided the section thickness and distortion problems by the following design. Estimates of the reference volume (V[r], made using the Cavalieri

principle) and particle numerical density (N[p]/V[r], made using physical disectors) were based on sections drawn from the same section set. By design, section thickness and tissue distortion were common to both estimates and cancelled out in the final calculation.

First a Cavalieri estimate of volume was obtained:

$$\text{est}\,V[r] = \Sigma P[r] \times a \times d$$

where ΣP[r] is the sum of test points, each with an areal equivalent a, falling on a uniform random sample of sections.

Secondly, a disector estimate of particle numerical density was calculated:

$$\text{est}\,N[p]/V[r] = \Sigma Q^{-}[p]/\Sigma P'[r] \times a' \times d$$

where ΣP′[r] is the sum of test points falling on the reference space of the disector frames and a′ is the areal equivalent of one of those points.

Next, the two estimators were combined:

$$\text{est}\,N[p] = (\Sigma P[r] \times a \times d) \times (\Sigma Q^{-}[p]/\Sigma P'[r] \times a' \times d)$$

$$= (a/a') \times (\Sigma P[r]/\Sigma P'[r]) \times \Sigma Q^{-}[p]$$

in order to obtain an unbiased estimate of particle number. This is similar to a fractionator equation (see below) but with estimated rather than known sampling fractions (see also Geiser et al. 1990).

The fractionator. This sampling approach circumvents technical sources of bias to provide direct estimates of number. It is not necessary to know specimen magnification, the area of the counting frame, section separation or the reference volume (whether fresh, fixed or fixed and embedded). What is required is random sampling in 3D space using known sampling fractions.

The volume in which structural features are contained can be cut systematically into random sections of arbitrary size, shape and number. However, the section planes should not intersect inside the objects if they are being employed to make disector pairs (Pakkenberg & Gundersen, 1988). The fraction, 1/f, of sections sampled in this way will contain n × f particles where n indicates the number counted in the sample. Often, the sample will comprise several disector pairs (when n is equal to Q^{-}) but, in certain circumstances, it is possible to use a point-like inclusion within a particle (e.g. the nucleolus inside a nucleus) for counting in sets of single sections (Braendgaard & Gundersen, 1986; Nairn et al. 1989; Mayhew, 1991*b*; Mwamengele et al. 1993).

The fractionator principle will usually be applied in several sampling stages with systematic sampling at each stage (Fig. 5). The number of particles is then estimated as

$$\text{est}\,N = n \times f1 \times f2 \times f3 \ldots \times fk$$

where fk is the sampling period (the reciprocal of the sampling fraction) at the lowest sampling stage. The number of stages, and the fraction selected at each, can be altered to suit best the requirements of a particular experiment. A reasonable workload is to design sampling so that n is approximately 100.

The specimen in which the particles are embedded may be divided quite arbitrarily at any stage except the last one. At the last stage, parallel sections are

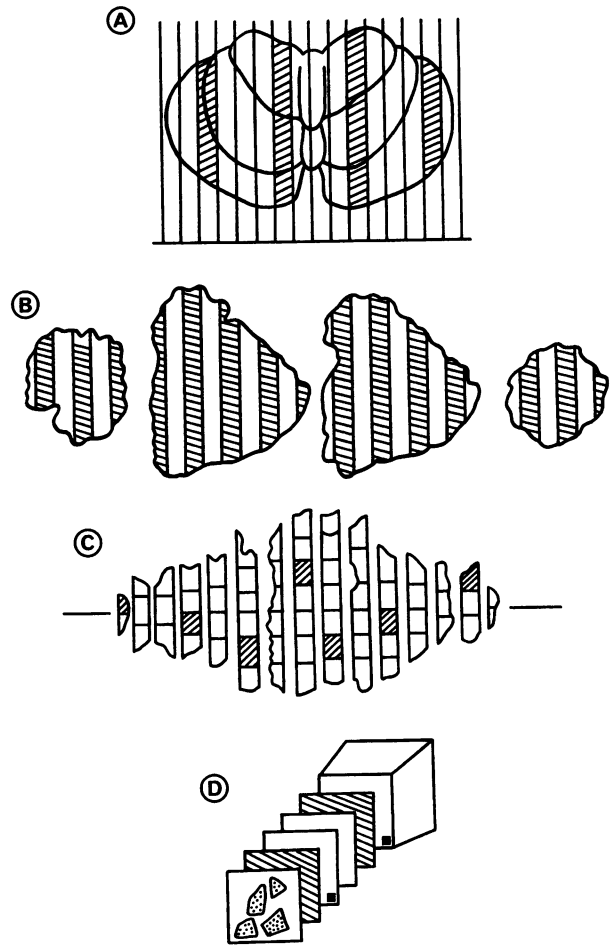

Fig. 5. The fractionator principle. In (A) an organ is cut into an exhaustive set of slices from which a known fraction, $\frac{1}{4}$, is drawn with a random start. In (B) the sampled slices are cut into strips from which an SR sample (fraction $\frac{1}{2}$) is selected. In (C) the selected strips are arranged in an artificial 'spindle' pattern from which an SR sample (fraction $\frac{1}{10}$) is taken. In (D) these are block-embedded and exhaustively serially sectioned so that a final SR sample (fraction $\frac{1}{3}$) can be drawn. Usually these will comprise disector pairs (reference shown hatched, look-up identified with a black square). Particles in the disector pairs are counted and their number is multiplied by the sequence $4 \times 2 \times 10 \times 3$ to estimate the total number in the entire organ. (Reproduced with permission from Mayhew, 1992).

advisable for technical reasons. Efficiency may be improved by cutting so that pieces contain roughly equal numbers of particles. For an organ in which the 3D spatial distribution of particles is rather uniform, this will be achievable by cutting into pieces of roughly equal size. However, it is generally preferable to arrange the specimen pieces produced at a given sampling stage into a series with a 'dome' or 'spindle' distribution. With this arrangement, the pieces at the ends of the series will be the smallest and those at the centre will be the biggest (see Ogbuihi & Cruz-Orive, 1990; Mayhew, 1992).

The dome distribution may arise naturally, at least at the first sampling stage. Thus a convex specimen cut into slices might generate a dome pattern if the slices are maintained in their natural order after slicing. Additional improvements in efficiency can be made by excising and discarding those regions of the specimen which do not contain the particles to be counted. For instance, the white matter and deep nuclei of the cerebellum do not contain Purkinje neurons and, if the size of the cerebellum permits, the cortex can be partly separated from subcortical tissue and discarded. This practice will not affect in any way the unbiasedness of the method.

Cruz-Orive (1990) has provided an improved method for predicting the variance of a fractionator estimate of number. At the initial stage of systematic sampling, the specimen is divided into two subsamples. Subsequently, the empirical variance of the pooled estimate of number is estimated using the pair of observations made on these two subsamples.

The double disector. It is sometimes desirable to count small objects inside, or otherwise associated with, larger objects. One way of achieving this aim, the 'double disector', has been employed to estimate numbers of synapses per neuron (Braendgaard & Gundersen, 1986; Gundersen et al. 1988*a*) and numbers of cells per renal glomerulus (Marcussen, 1992*a*). In the former example, the numerical densities of synapses and neurons were determined in the same set of ultrathin sections. By estimating neuron number from semithin sections, the absolute number of synapses was calculated.

Double disectors have been employed to count the numbers of coated vesicles and their precursors (coated pits) per nucleus during endocytosis of ^{125}I-transferrin by broken A431 cells (Smythe et al. 1989). More recently, Lucocq (1992) has used double disectors to count immunogold particles per cell at the ultrastructural level. He combined these stereological data with biochemical estimates of antigens per cell in order to determine labelling efficiency, an important experimental variable in modern immuno-electron microscopy.

SOME APPLICATIONS

To date, modifications of the disector have been used to count a variety of different sorts of particle. For convenience, the 'particles' may be classified as falling into 3 main groups: (1) discrete particles such as cells, nuclei, synapses, intracellular vesicles, (2) associated features of particles such as gland/pore openings, mouths of forming endosomes, bases of microvilli, synaptic membrane densities, and (3) connected sets such as capillary networks, Golgi stacks and interconnected pores.

Many of the applications involve counting neurons and synapses (Gundersen, 1985; Braendgaard & Gundersen, 1986; Pakkenberg & Gundersen, 1988; Mayhew, 1992; West, 1993*a*), reflecting the keen interest of neurobiologists in one of the two principal areas in which number offers useful information, i.e. intercellular communication and connectivity (Mayhew et al. 1979). Combined with immunochemical staining, it is now possible to count defined subsets of neurons (e.g. Janson & Møller, 1993; Aika et al. 1994). Studies also reflect the other main area, i.e. that of genesis, growth and transformation, in which number helps us to understand mechanisms of particle formation, to distinguish between hyperplastic, hypertrophic and interstitial growth, and to explore mechanisms of cell/tissue differentiation. The following application summary is meant to be illustrative rather than comprehensive.

Optical disectors

There are now many reports of the use of the optical disector in thin-focus microscopy to count neurons, glial and other cells in mammalian and avian central and peripheral nervous systems. These include studies of sex and age differences, patterns of development, the effects of alcoholism, senile dementia of Alzheimer type, growth factors and other forms of experimental manipulation and possible novel therapeutic interventions for Parkinson's disease. Particles counted include neurons, glial, ependymal and endothelial cells in the spinal cord (Bjugn, 1991, 1993; Bjugn & Gundersen, 1993), neurons in lumbar dorsal root ganglia (Tandrup, 1993; Tandrup & Braendgaard, 1994), cerebral cortex (Pakkenberg et al. 1989; Braendgaard et al. 1990; Tandrup & Braendgaard, 1992; Jensen & Pakkenberg, 1993; Regeur et al. 1994), neurons and glial cells in substantia nigra (Janson & Møller, 1993), neurons in the lumbar

lateral motor column (Nurcombe et al. 1991) and in the hippocampus and its subregions (West & Gundersen, 1990; West et al. 1991; Holm & West, 1993; West, 1993*b*).

Optical disectors have also been used to count and size mesophyll cells in leaves of barley plants (Kubinova, 1989) and to count osteocyte lacunae by confocal microscopy (Howard et al. 1985) and total number of cells per renal glomerulus by thin-focus microscopy (Bertram et al. 1992).

Physical disectors

Apart from examples embedded in review articles (Braendgaard & Gundersen, 1986; Gundersen et al. 1988*a*), physical disectors have been applied to various particle types.

In the case of discrete particles, they have been used to count and size neurons in the cerebral cortex of control and undernourished rats (Møller et al. 1990; Korbo et al. 1990; Bedi 1994), rat brainstem (Guntinas-Lichius et al. 1993), dentate gyrus (West et al. 1988; Bedi, 1991), superior colliculus (Fukui & Bedi, 1991) and CA1 region of rat hippocampus (Aika et al. 1994). Pakkenberg and colleagues have counted neurons and glial cells in the brains of diseased subjects including schizophrenics and Parkinson's disease sufferers (Pakkenberg & Gundersen, 1988, 1989; Pakkenberg, 1990; Pakkenberg et al. 1991). They have demonstrated reduced numbers of neurons, astrocytes and oligodendroglial cells in the mediodorsal thalamic nucleus and nucleus accumbens in schizophrenics but no differences in the ventral pallidum or basolateral nucleus of the amygdala. Total neuron number in Parkinson's patients was 66% less than in control subjects.

Nuclei in malignant and benign melanocytic skin tumours have been counted in physical disectors (Sørensen, 1991) and used to estimate the variance of the distribution of nuclear volumes. Mendis-Handagama (1992) employed disectors to estimate numbers of Leydig cells in rat testes and to quantify the biases introduced by model-based methods. The authors emphasised that biased (model and shrinkage-dependent) estimates of number were similar to unbiased estimates in control but not experimentally induced atrophic testes. However, the real lesson to be learned is that biased methods do not *in general* give unbiased estimates. Numbers of parathyroid cells have been determined in hypercalcaemic rats and in onset and age-matched controls (Wernerson et al. 1989). Total numbers of secretory cells increased in controls by 100% from 3 to 7 wk. The reduced cell number and size in hypercalcaemic rats reflected growth arrest rather than atrophy. Bertram et al. (1992) used TEM physical disectors to count different cell types in glomeruli of normal rat kidney as a baseline for comparative studies on various renal disorders.

Several groups have examined tissue/organ growth by testing for hyperplasia and other strategies. Hyperplasia versus hypertrophy in smooth muscle cells of mesenteric resistance vessels of spontaneously hypertensive rats has been examined (Baandrup et al. 1985; Mulvany et al. 1985). It was found that hyperplasia is the basis of the thickened tunica media in such vessels. Mayhew and colleagues (Simpson et al. 1992; Mayhew & Simpson, 1994; Mayhew et al. 1994*b*) counted nuclei in different tissue compartments of human placental villi during gestation and found that whilst nuclei in all compartments increased in the same (logarithmic) fashion, overall growth strategies differed. In the trophoblast, growth was purely hyperplastic and occurred by the continuous recruitment of new proliferative units. There was no depletion of cytotrophoblast cells, thus contradicting the impression of a decline given by sectional images. The apparent decline can be explained by the relatively greater expansion of villus surface area and thinning of trophoblastic epithelium.

Other discrete particles counted include type II pneumocytes in control and ozone-exposed rats (Dormans, 1989), immunogold particles in labelled cells (Lucocq, 1992) and pores in aluminium and in sandstone (Karlsson & Cruz-Orive, 1992; Zhao & MacDonald, 1993). Mandarim-de-Lacerda & Costa (1993) monitored myocyte packing density in different parts of the myocardium. The highest packing was found in the crista terminalis and atrioventricular bundle followed by the interatrial and interventricular septa. Austin et al. (1995) devised a method for estimating numbers of ventricular myocyte nuclei in fetal and postnatal hearts. Their findings suggest that postnatal growth is not hyperplastic and that patterns of growth are similar in left and right ventricles. Marcussen and colleagues (Marcussen & Olsen, 1989; Marcussen, 1990, 1991, 1992*b*; Marcussen & Jacobsen, 1992) counted glomeruli in patients with various types of renal pathology. Schmitz et al. (1990) used physical disectors as a basis for estimating glomerular volume in type 2 diabetes.

In the case of associated features, so far these have been confined mainly to presynaptic membrane densities and to invaginating coated vesicles during endocytosis. However, disectors could be used to

count microvillus bases and, thereby, offer an unbiased way of tackling the problem of distinguishing ambiguous profiles of microvilli at apposed cell surfaces (Mayhew, 1985).

Synapses of various types (perforated and non-perforated, symmetric and asymmetric) have been counted in the rat superior colliculus after dark-rearing (Fukui & Bedi, 1991) and in the neocortex (Calverley & Jones, 1987, 1990; Calverley et al. 1988). De Groot & Bierman (1986, 1987) found a significant decrease in numbers of nonperforated synapses in the stratum radiatum of hippocampal C3 area in female rats between 3 and 24 months but no significant decrease in perforated synapses. Siklos et al. (1990) showed that numbers of synapses in the superior cervical ganglion did not change after long-lasting administration of the membrane hyperpolarising agent, sodium bromide.

Studies on the chick lobus parolfactorius (Hunter & Stewart, 1989) have shown that the numerical density of all classes of synapses increases with age (16 d prehatch to 22 d posthatch) but the proportion of symmetric synapses rises. There was hemisphere asymmetry in asymmetric synapses posthatch, the left hemisphere containing relatively more asymmetric spine synapses per volume.

In cultured cells undergoing endocytosis, coated pits (the precursors of coated vesicles) depend on the addition of cytosol and ATP for their formation (Smythe et al. 1989).

For connected sets of 'particles', physical disectors have been used, most notably, to count capillaries (Nyengaard et al. 1988; Nyengaard & Marcussen, 1993). The term capillary unit is first given a rigorous topological definition and then used to count capillary units in renal glomeruli during normal development, nephrectomy and experimental diabetes (Nyengaard et al. 1988, 1993; Nyengaard & Bendtsen, 1992; Nyengaard, 1993*a*, *b*; Nyengaard & Rasch, 1993). Results suggest that capillary branching, forming a complex net of serial and parallel connections, is the structural basis for normal growth of glomerular capillaries from 5 d to 8 months postnatally. Lucocq et al. (1989) counted Golgi clusters and vesicles in dividing (metaphase) HeLa cells and during telophase Golgi reassembly. They found thousands of free vesicles in metaphase which shifted to clusters during telophase, suggesting an economical mechanism for replication of the Golgi apparatus during cell division.

The above estimates are based on the fact that for arbitrary networks, the disector provides an unbiased estimate of the so-called Euler-number (Gundersen et al. 1993), which has been used in a series of studies of bone trabecular connectivity by R. W. Boyce (Youngs et al. 1994; Boyce et al. 1995).

Fractionators

Applications of the fractionator to count particles in optical and physical sections are increasingly common. Again, most are based on neurons and glial cells in different regions of the nervous system (Braendgaard & Gundersen, 1986; Pakkenberg & Gundersen, 1988; West et al. 1991). In the case of cerebellar Purkinje cells, these have been examined with regard to age, sex, nutritional status, lateral symmetry and phylogeny (Nairn et al. 1989; Mayhew et al. 1990; Andersen et al. 1992; Bedi et al. 1992; Korbo et al. 1993). For adult terrestrial mammals at least, it seems that cerebellar weight correlates very well with the Purkinje complement and offers a simple way of predicting number (Mayhew, 1991*b*; Mwamengele et al. 1993).

Two studies on lung have adopted the fractionator principle: the one to count macrophages in, and particles retained in and cleared from, the intrapulmonary conducting airways of hamsters (Geiser et al. 1989, 1990, 1994) and the other to count the total number of lymphatic valves in human infants (Ogbuihi & Cruz-Orive, 1990). Leydig cells in rat testes have been counted (Mendis-Handagama, 1992) as have renal glomeruli in normal rats and human diabetic patients (Bendtsen & Nyengaard, 1992; Bertram et al. 1992). Wigmore et al. (1992) used a combination of the disector and fractionator sampling to show that nuclear number increases during development of lumbrical muscle IV in the rat (E17 to 3 months postpartum). The proportion of fibre nuclei increased as cells fused to form secondary fibres. At the same time, the proportion of nuclei of myogenic precursor cells declined whilst that of connective tissue nuclei did not alter markedly.

SAMPLING FOR PARTICLE SIZING

Once a method is available for counting particles in an unbiased manner, that method will also permit unbiased *selection* of particles for other purposes. Thus a direct consequence of the disector is the availability of a procedure for selecting particles for size estimation. Size may be defined in various ways (e.g. volume, surface area, height) and most estimators of mean size can be obtained by dividing total (or relative) volume, surface or height by total (or relative) number. In most instances, however, volume is the most informative definition of size and so this section

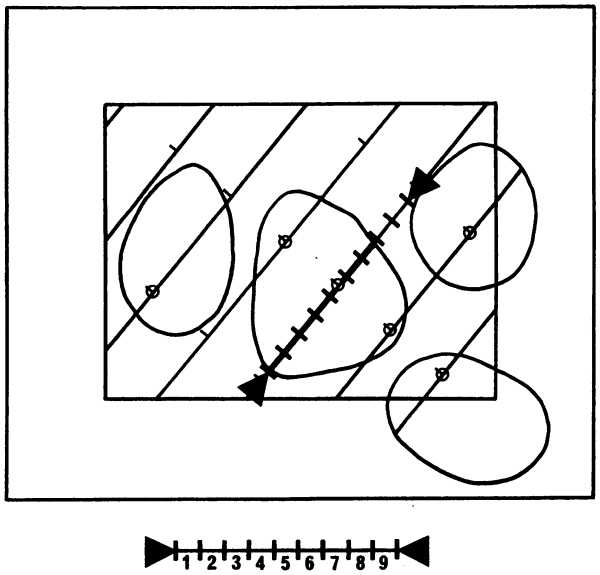

Fig. 6. Volume estimation from point-sampled intercept (PSI) lengths. A set of particle profiles appears on a single section on which is superposed a frame with a surrounding guard area. The frame contains a set of randomly oriented test lines bearing test points of which 6 (open circles) fall on the profiles and lie inside the frame. The lengths of PSIs which cross the profiles and pass through the points are estimated using a graduated scale. The PSI shown falls in class 7 of the scale. If line directions are isotropic in 3D, the PSIs through all 6 points provide an unbiased estimate of the volume-weighted mean volume of the particles. By first selecting particles with disector pairs, the same procedure will generate a number-weighted mean volume. (Reproduced by permission from Mayhew, 1992).

briefly reviews three volume estimation procedures for estimating the sizes of individual particles.

The selector

This device (Cruz-Orive, 1987*a*) may be regarded as combining the disector (for selecting arbitrary features with identical probabilities, i.e. a uniform random sample) and point-sampled intercept (PSI) length measurement (for estimating feature volume, Fig. 6). Because features are selected with identical probabilities (based merely on their presence), the resulting estimates are direct estimates of number-weighted rather than volume-weighted volumes. Moreover, this is achieved without knowing the distance between the two planes, i.e. the selector is a disector of unknown thickness.

First, stacks of serial sections are cut. These may be isotropic uniform random (IUR) sections generated in 3D using the orientator or isector (Mattfeldt et al. 1990; Nyengaard & Gundersen, 1992) or in 2D by vertical sectioning (Baddeley et al. 1986). Next, a disector pair from each set is drawn so as to select features solely according to their presence. The number-weighted mean volume of the chosen features is obtained from their PSI lengths by superimposing test points on all sections through the features. Independently, intercepts are measured along test lines which pass through the points. The test lines must be IUR in 3D space, hence the need to cut IUR sections or to cut vertical sections and apply sine-weighted test lines (Baddeley et al. 1986; Cruz-Orive & Hunziker, 1986; Gundersen et al. 1988*a*, *b*). If the features are convex, the intercepts will be connected segments of length l_0. An unbiased estimate of number-weighted volume, v_N, is obtained by averaging the third power of PSI lengths over all intercepts and multiplying by $(\pi/3)$. Additional steps must be taken if features are non-convex. A value of v_N is obtained for each sampled feature and then averaged to give the number-weighted mean volume for the sampled set (Cruz-Orive, 1987*a*).

Sections from the selector set can be used to calculate particle volume in the volume-weighted distribution of volume (Gundersen & Jensen, 1985). By combining this with number-weighted volume, information about size variation (the coefficient of variation of volume in the number distribution) can be obtained. Moreover, this can be achieved without needing to know or reconstruct the actual volume-frequency distribution.

Ependymal cells in spinal medulla (Bjugn et al. 1989), cells in skin tumours (McMillan & Sørensen, 1992), human erythrocytes (Mayhew et al. 1994*a*) and pores in sand-cast aluminium alloys (Karlsson & Cruz-Orive, 1992) have been sized using the selector.

The nucleator

This is similar to the selector but is a more efficient way of estimating number-weighted mean volume when particles possess a single identifiable point-like inclusion (Gundersen, 1988). At the cellular level, an ideal inclusion is the nucleolus. The increased efficiency arises by virtue of the fact that, in order to estimate mean volume, only those sections which contain the inclusion need to be sampled.

The nucleator relies on a generalisation of a special case which we were all taught in school, i.e. the method for calculating the volume of a sphere:

$$V = 4\pi r^3/3$$

where r is the sphere radius. In this model-based case, volume is determined by measuring from a central point to the sphere boundary. In fact, the point may be located anywhere inside or outside the sphere and, provided that IUR lines in 3D space are used to define directions from the point to the boundary, the method is applicable to arbitrary particles (Gundersen, 1988).

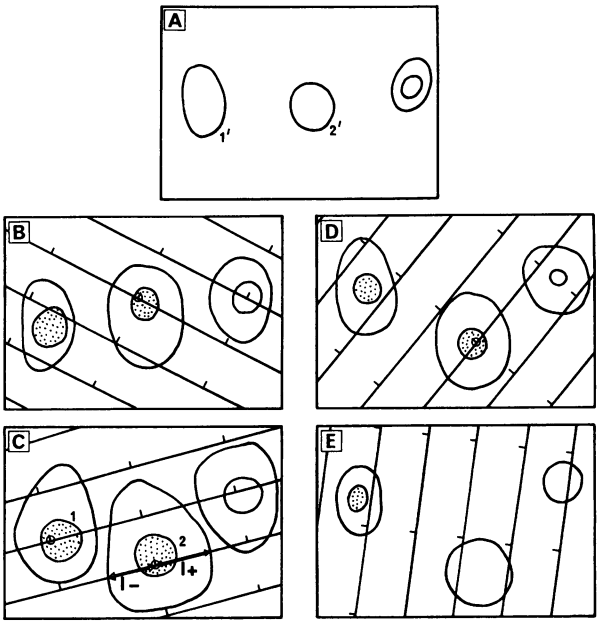

Fig. 7. Cell volume estimation with the nucleator. (A–E) represents a set of serial sections through 3 cells, each containing a single nucleus. The disector pair (A) (look-up), (C) (reference) is used to sample nuclei solely according to their presence. On this basis, 2 nuclei (1, 2) appear on (C) but not on (A) (see cell profiles 1′2′). These nuclei are followed through the section stack (stippled). An overlay of lines (isotropic in 3D) is superposed on these sections and some points hit the selected nuclei (4 open circles). Distances from the points to the cell boundary (see l^+ and l^-) are used to estimate number-weighted mean volume. (Reproduced with permission from Mayhew, 1992).

For reasons of efficiency, it is sensible to confine the point to within the particle itself.

Imagine a population of cells, each containing a single nucleolus, for which an estimate of mean cell volume is required (Fig. 7). As with the selector, we begin by cutting a stack of sections but, in contrast to the selector, this need only be as high as the linear dimension of the largest nucleolus (measured at right angles to the section plane). Having sampled nucleoli with identical probabilities (by using a disector from the section stack), test points are applied to every section which contains profiles of those nucleoli. For each point hitting a nucleolar profile, an isotropic direction is chosen in order to draw a line from the point to the boundary of the cell profile.

An unbiased estimate of number-weighted mean volume for the cells is calculated by averaging, over all intercepts, the third powers of intercept lengths and multiplying this average by $4\pi/3$ (Gundersen, 1988). If lines are drawn across the cell profiles, passing through the chosen points, then two possible intercepts may be measured, each passing from the point to the cell profile boundary. Estimates of cell volume can be made using either or both of these intercepts (Jack et al. 1990*a*, *b*).

It is helpful to note that if a single small nucleolus of approximately constant size is adopted as the inclusion, the number-weighted mean volume of cells can be estimated from just one section or from several independent sections (Gundersen, 1988). Various illustrations of the use of the nucleator are available (Gundersen et al. 1988*a*, *b*; Bagger et al. 1989, 1993; Jack et al. 1990*a*, *b*; Møller et al. 1990), including some which illustrate how the distribution of volumes (Andersen et al. 1992; Strange et al. 1991) and the spatial distribution (Evans & Gundersen, 1989) of individual cell bodies may be analysed.

The rotator

As with the nucleator, this principle (Cruz-Orive, 1987*b*; Vedel Jensen & Gundersen, 1993) relies on a unique point-like reference (e.g. a nucleolus) being associated with each particle. It, too, offers unbiased number-weighted volume estimates when used on vertical sections (the vertical rotator, Cruz-Orive, 1987*b*) or on sections which are IUR in 3D space (the isotropic rotator, Vedel Jensen & Gundersen, 1993). However, the method is likely to be more precise than the nucleator.

Sampling requirements are the same as for the nucleator. We begin by cutting a stack of sections as high as the linear dimension of the largest nucleolus so as to sample nucleoli with identical probabilities. A lattice of parallel test lines, separated by a distance t, is applied to every cell section which contains a nucleolar profile. A convenient design is to set t as h/3 where h is the apparent cell height in the vertical direction (vertical rotator) or in a chosen IUR direction (isotropic rotator).

In the case of vertical sectioning (see Fig. 8), the lattice is positioned so that a vertical axis (orthogonal to the test lines) passes through the nucleolus. It is not a precondition that one of the test lines should intercept the nucleolus. For each test line crossing the cell, linear intercepts from this axis to the cell boundary are measured on both sides of the vertical axis. Particle volume is estimated for each cell by squaring the intercepts measured on both sides of each test line, taking their mean, and then summing over all test lines. This value, Σl_i^2, multiplied by $\pi \cdot t$, is an unbiased estimate of the number-weighted volume of that cell. Mean cell volume is obtained by averaging over all selected cells (Vedel Jensen & Gundersen, 1993).

With the isotropic rotator, lattices are positioned so that a chosen IUR direction passes through the nucleolus. Moreover, volume estimation requires

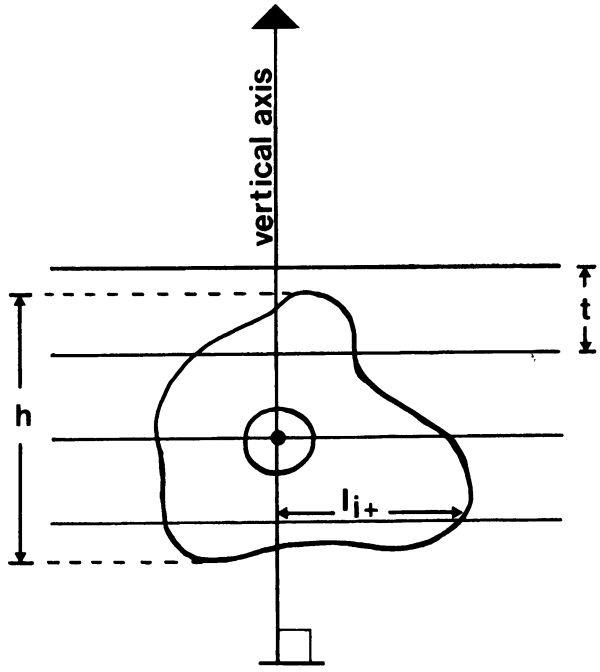

Fig. 8. The vertical rotator to estimate cell volume. Nucleoli within cells are sampled, as with the nucleator, according to their presence. A lattice of parallel test lines, distance t apart, is applied to every cell section which contains a nucleolar profile. It is not a requirement that one of these lines should intercept the nucleolus (black circle) but the lattice must be positioned so that its vertical axis passes through the nucleolus. For each test line crossing the cell (height h), linear intercepts from this axis to the cell boundary are measured on both sides of the vertical axis. Only one such intercept (l_{i+}) is indicated. The number-weighted cell volume is estimated for each cell after squaring the intercepts measured on both sides of each vertical axis, taking their mean, and then summing over all test lines.

additional information about distances from each test line to the nucleolar centre. In fact, volume is obtained using the estimator $2.t.\Sigma g_i$, where Σg_i is a function of the intercept lengths and the nucleolus-vertical axis distances (for details, see Vedel Jensen & Gundersen, 1993).

Examples of applications to neuron populations are offered in Vedel Jensen & Gundersen (1993). Janson & Møller (1993) have used the rotator to estimate the volumes of neurons and glial cells in rat substantia nigra. They showed that, following partial midbrain hemisection, chronic nicotine infusion had a selective protective effect on loss of nigral dopamine neurons.

CONCLUDING REMARKS

The disector principle has revolutionised the scientific basis of particle counting and sizing from sections. Since Science advances in part by the development of better techniques, the application of the earlier assumption or model-dependent methods should be discontinued unless firm evidence can be adduced, for each and every application, that their use is fully justified. We should no longer accept the excuse that 'We used model-based methods because we needed to compare our results with earlier findings'. This pays homage to History not Science. It is also important to appreciate that unbiasedness in general is a built-in property of design-based methods. What works for a potato or a carrot or a coin will also work for a synapse or a polymorph nucleus or a myocyte or whatever. Consequently, there is no need to waste time by the wholly redundant exercise of 'testing' these methods on artificial models.

ACKNOWLEDGEMENTS

The idea for this review was conceived on a train to Zürich following a meeting in Bern to mark the retirement of Ewald Weibel. We wish to thank the organisers of that meeting for its success and for providing the opportunity for us to discuss this review and to plan it further at Zürich airport. We also gratefully acknowledge the help, stimulation, collaboration and friendship offered by our many colleagues worldwide. This includes Luis Cruz-Orive (Santander) who, as a named referee, provided many useful ideas for improving the manuscript.

REFERENCES

AIKA Y, REN JQ, KOSAKA Y, KOSAKA T (1994) Quantitative analysis of GABA-like-immunoreactive and parvalbumin-containing neurons in the CA1 region of the rat hippocampus using a stereological method, the disector. *Experimental Brain Research* **99**, 267–276.

ANDERSEN BB, KORBO L, PAKKENBERG B (1992) Quantitative study of the human cerebellum using unbiased stereological techniques. *Journal of Comparative Neurology* **326**, 549–560.

AUSTIN A, FAGAN DG, MAYHEW TM (1995) A stereological method for estimating the total number of ventricular myocyte nuclei in fetal and postnatal hearts. *Journal of Anatomy*, **187**, 641–647.

BAANDRUP U, GUNDERSEN HJG, MULVANY MJ (1985) Is it possible to solve the problem: hypertrophy/hyperplasia of smooth muscle cells in the vessel wall of hypertensive subjects? *Progress in Applied Microcirculation* **8**, 122–128.

BADDELEY AJ, GUNDERSEN HJG, CRUZ-ORIVE L-M (1986) Estimation of surface area from vertical sections. *Journal of Microscopy* **142**, 259–276.

BAGGER PV, BANG L, CHRISTIANSEN MD, KABELL-KJAER E, MORTENSEN E, GUNDERSEN HJG (1989) Classification of isolated ovarian follicles using the nucleator: estimation of antral volume. *Acta Stereologica* **8**, 123–126.

BAGGER PV, BANG L, CHRISTIANSEN MD, GUNDERSEN HJG, MORTENSEN E (1993) Total number of particles in a bounded region estimated directly with the nucleator: granulosa cell number in ovarian follicles. *American Journal of Obstetrics and Gynecology* **168**, 724–731.

BEDI KS (1987) A simple method of measuring the thickness of semi-thin and ultra-thin sections. *Journal of Microscopy* **148**, 107–111.

BEDI KS (1991) Effects of undernutrition during early life on granule cell numbers in the rat dentate gyrus. *Journal of Comparative Neurology* **211**, 425–433.

BEDI KS (1994) Undernutrition of rats during early life does not

affect the total number of cortical neurons. *Journal of Comparative Neurology* **342**, 596–602.

BEDI KS, CAMPBELL LF, MAYHEW TM (1992) A fractionator study of the effects of undernutrition during early life on rat Purkinje cell numbers (with a caveat on the use of nucleoli as counting units). *Journal of Anatomy* **181**, 199–208.

BENDTSEN TF, NYENGAARD JR (1989) Unbiased estimation of particle number using sections—an historical perspective with special reference to the stereology of glomeruli. *Journal of Microscopy* **153**, 93–102.

BENDTSEN TF, NYENGAARD JR (1992) The number of glomeruli in insulin-dependent and non-insulin-dependent diabetic patients. *Diabetologia* **35**, 844–850.

BERTRAM JF, SOOSAIPILLAI MC, RICARDO SD, RYAN GB (1992) Total numbers of glomeruli and individual glomerular cell types in the normal rat kidney. *Cell and Tissue Research* **270**, 37–45.

BJUGN J (1991) Estimation of the total number of cells in the rat spinal cord using the optical disector. *Micron and Microscopica Acta* **22**, 25–26.

BJUGN J (1993) The use of the optical disector to estimate the number of neurons, glial and endothelial cells in the spinal cord of the mouse—with a comparative note on the rat spinal cord. *Brain Research* **627**, 25–33.

BJUGN J, BOE R, HAUGLAND HK (1989) A stereological study of the ependyma of the mouse spinal cord. With a comparative note on the choroid plexus ependyma. *Journal of Anatomy* **166**, 171–178.

BJUGN J, GUNDERSEN HJG (1993) Estimate of the total number of neurons and glial and endothelial cells in the rat spinal cord by means of the optical disector. *Journal of Comparative Neurology* **328**, 406–414.

BOYCE RW, EBERT DC, YOUNGS TA, PADDOCK CL, MOSEKILDE L, STEVENS ML, GUNDERSEN HJG (1995) Unbiased estimation of vertebral trabecular connectivity in calcium-restricted ovariectomized minipigs. *Bone* **16**, in press.

BRAENDGAARD H, GUNDERSEN HJG (1986) The impact of recent stereological advances on quantitative studies of the nervous system. *Journal of Neuroscience Methods* **18**, 39–78.

BRAENDGAARD H, EVANS SM, HOWARD CV, GUNDERSEN HJG (1990) The total number of neurons in the human neocortex unbiasedly estimated using optical disectors. *Journal of Microscopy* **157**, 285–304.

CALVERLEY RKS, JONES DG (1987) Determination of the numerical density of perforated synapses in rat neocortex. *Cell and Tissue Research* **248**, 399–407.

CALVERLEY RKS, BEDI KS, JONES DG (1988) Estimation of the numerical density of synapses in rat neocortex. Comparison of the 'disector' with an 'unfolding' method. *Journal of Neuroscience Methods* **23**, 195–205.

CALVERLEY RKS, JONES DG (1990) Determination of numerical density of perforated and nonperforated synapses. In *Methods in Neurosciences*, vol. 3, *Quantitative and Qualitative Microscopy* (ed. P. M. Conn), pp. 155–172. London: Academic Press.

CRUZ-ORIVE L-M (1980) On the estimation of particle number. *Journal of Microscopy* **120**, 15–27.

CRUZ-ORIVE L-M (1987*a*) Particle number can be estimated using a disector of unknown thickness: the selector. *Journal of Microscopy* **145**, 121–142.

CRUZ-ORIVE L-M (1987*b*) Stereology: recent solutions to old problems and a glimpse into the future. *Acta Stereologica* **6**, 3–18.

CRUZ-ORIVE L-M (1990) On the empirical variance of a fractionator estimate. *Journal of Microscopy* **160**, 89–95.

CRUZ-ORIVE L-M, HUNZIKER EB (1986) Stereology for anisotropic cells: application to growth cartilage. *Journal of Microscopy* **143**, 47–80.

CRUZ-ORIVE L-M, WEIBEL ER (1990) Recent stereological methods for cell biology: a brief survey. *American Journal of Physiology* **258**, L148–156.

DE GROOT DMG (1988) Comparison of methods for the estimation of the thickness of ultrathin tissue sections. *Journal of Microscopy* **151**, 23–42.

DE GROOT DMG, BIERMAN EPB (1986) A critical evaluation of methods for estimating the numerical density of synapses. *Journal of Neuroscience Methods* **18**, 79–101.

DE GROOT DMG, BIERMAN EPB (1987) Numerical changes in rat hippocampal synapses. An effect of 'ageing'? *Acta Stereologica* **6**, 53–58.

DORMANS JAM (1989) Application of the disector method in the light microscopic quantification of the type II pneumocytes in control and ozone-exposed rats. *Journal of Microscopy* **155**, 207–211.

EVANS SM, GUNDERSEN HJG (1989) Estimation of spatial distributions using the nucleator. *Acta Stereologica* **8**, 395–401.

EVANS SM, HOWARD CV (1989) A simplification of the 'step' method for estimating mean section thickness. *Journal of Microscopy* **154**, 289–293.

FUKUI Y, BEDI KS (1991) Quantitative study of the development of neurons and synapses in rats reared in the dark during early postnatal life. 1. Superior colliculus. *Journal of Anatomy* **174**, 49–60.

GEISER M, CRUZ-ORIVE L-M, HOF VI, GEHR P (1989) Counting particles retained in the conducting airways of hamster lungs with the fractionator. *Acta Stereologica* **8**, 419–424.

GEISER M, CRUZ-ORIVE L-M, HOF VI, GEHR P (1990) Assessment of particle retention and clearance in the intrapulmonary conducting airways of hamster lungs with the fractionator. *Journal of Microscopy* **160**, 75–88.

GEISER M, BAUMANN M, CRUZ-ORIVE L-M, HOF VI, WABER U, GEHR P (1994) The effect of particle inhalation on macrophage number and phagocytic activity in the intrapulmonary conducting airways of hamsters. *American Journal of Respiratory Cell and Molecular Biology* **10**, 594–603.

GOLDSTEIN DJ, HARTMANN-GOLDSTEIN IJ (1974) Accuracy and precision of a scanning and integrating microinterferometer. *Journal of Microscopy* **102**, 143–164.

GUNDERSEN HJG (1977) Notes on the estimation of the numerical density of arbitrary profiles: the edge effect. *Journal of Microscopy* **111**, 219–223.

GUNDERSEN HJG (1985) Quantitative analysis of three-dimensional structures in neuroanatomy. In *Quantitative Neuroanatomy in Transmitter Research* (ed. L. F. Agnati & K. Fuxe), pp. 3–9. Basingstoke and London: MacMillan Press.

GUNDERSEN HJG (1986) Stereology of arbitrary particles. A review of unbiased number and size estimators and the presentation of some new ones, in memory of William R. Thompson. *Journal of Microscopy* **143**, 3–45.

GUNDERSEN HJG (1988) The nucleator. *Journal of Microscopy* **151**, 3–21.

GUNDERSEN HJG, ANDERSEN BS, FLOE H (1983) Estimation of section thickness unbiased by cutting deformation. *Journal of Microscopy* **131**, RP3–RP4.

GUNDERSEN HJG, JENSEN EB (1985) Stereological estimation of the volume-weighted mean volume of arbitrary particles observed on random sections. *Journal of Microscopy* **138**, 127–142.

GUNDERSEN HJG, JENSEN EB (1987) The efficiency of systematic sampling in stereology and its prediction. *Journal of Microscopy* **147**, 229–263.

GUNDERSEN HJG, BAGGER P, BENDTSEN TF, EVANS SM, KORBO L, MARCUSSEN N et al. (1988*a*) The new stereological tools: disector, fractionator and point-sampled intercepts and their use in pathological research. *Acta Pathologica et Microbiologica Scandinavica* **96**, 857–881.

GUNDERSEN HJG, BENDTSEN TF, KORBO L, MARCUSSEN N, MØLLER A, NIELSEN K et al. (1988*b*) Some new, simple and efficient stereological methods and their use in pathological research and diagnosis. *Acta Pathologica et Microbiologica Scandinavica* **96**, 379–394.

GUNDERSEN HJG, BOYCE RW, NYENGAARD JR, ODGAARD A (1993) The conneuler: unbiased estimation of connectivity using physical dissectors under projection. *Bone* **14**, 217–222.

GUNTINAS-LICHIUS O, MOCKENHAUPT J, STENNERT E, NEISS WF (1993) Simplified nerve cell counting in the rat brainstem with the physical disector using a drawing-microscope. *Journal of Microscopy* **172**, 177–180.

HARRIS T (1991) *The Silence of the Lambs*. London: Mandarin Paperbacks.

HOLM IE, WEST MJ (1993) The hippocampus of the domestic pig: a stereological study of subdivisional volumes and neuron numbers. *Hippocampus* **3**, 1–11.

HOWARD CV, REID S, BADDELEY AJ, BOYDE A (1985) Unbiased estimation of particle density in the tandem scanning reflected light microscope. *Journal of Microscopy* **138**, 203–212.

HUNTER A, STEWART MG (1989) A quantitative analysis of the synaptic development of the lobus parolfactorius of the chick (Gallus domesticus). *Experimental Brain Research* **78**, 425–434.

JACK EM, BENTLEY P, BIERI F, MUAKKASSAH-KELLY SF, STAUBLI W, SUTER J et al. (1990*a*) Increase in hepatocyte and nuclear volume and decrease in the population of binucleated cells in preneoplastic foci of rat liver: a stereological study using the nucleator method. *Hepatology* **11**, 286–297.

JACK EM, STAUBLI W, WAECHTER F, BENTLEY P, SUTER J, BIERI F et al. (1990*b*) Ultrastructural changes in chemically induced preneoplastic focal lesions in the rat liver: a stereological study. *Carcinogenesis* **11**, 1531–1538.

JANSON AM, MØLLER A (1993) Chronic nicotine treatment counteracts nigral cell loss induced by a partial mesodiencephalic hemitransection: an analysis of the total number and mean volume of neurons and glia in substantia nigra of the male rat. *Neuroscience* **57**, 931–941.

JENSEN EB, SUNDBERG R (1986) Generalized associated point methods for sampling planar objects. *Journal of Microscopy* **144**, 55–70.

JENSEN GB, PAKKENBERG B (1993) Do alcoholics drink their neurons away? *Lancet* **342**, 1201–1204.

KARLSSON LM, CRUZ-ORIVE L-M (1992) The new stereological tools in metallography: estimation of pore size and number in aluminium. *Journal of Microscopy* **165**, 391–415.

KORBO L, PAKKENBERG B, LADEFOGED O, GUNDERSEN HJG, ARLIEN-SOBORG P, PAKKENBERG H (1990) An efficient method for estimating the total number of neurons in rat brain cortex. *Journal of Neuroscience Methods* **31**, 93–100.

KORBO L, ANDERSEN BB, LADEFOGED O, MØLLER A (1993) Total numbers of various cell types in rat cerebellar cortex estimated using an unbiased stereological method. *Brain Research* **609**, 262–268.

KUBINOVA L (1989) Stereological analysis of the leaf of barley. *Acta Stereologica* **8**, 19–26.

LAROYE GJ, TAYLOR WB (1992) An acoustic depth alarm device to monitor vertical translation of the microscope stage: a practical optical disector, selector and unbiased brick for routine light microscopy. *Journal of Microscopy* **167**, 279–286.

LUCOCQ J (1992) Quantitation of gold labelling and estimation of labeling efficiency with a stereological counting method. *Journal of Histochemistry and Cytochemistry* **40**, 1929–1936.

LUCOCQ JM, BERGER EG, WARREN G (1989) Mitotic Golgi fragments in HeLa cells and their role in the reassembly pathway. *Journal of Cell Biology* **109**, 463–474.

MANDARIM DE LACERDA CA, COSTA WS (1993) An update of the stereology of the myocyte of the baboon's heart: analysis of the crista terminalis, interatrial and interventricular septa, and atrioventricular bundle. *Annals of Anatomy* **175**, 65–70.

MARCUSSEN N (1990) Atubular glomeruli in cisplatin-induced chronic interstitial nephropathy. An experimental stereological investigation. *Acta Pathologica et Microbiologica Scandinavica* **98**, 1087–1097.

MARCUSSEN N (1991) Atubular glomeruli in renal artery stenosis. *Laboratory Investigation* **65**, 558–565.

MARCUSSEN N (1992*a*) The double disector: unbiased stereological estimation of the number of particles inside other particles. *Journal of Microscopy* **165**, 417–426.

MARCUSSEN N (1992*b*) Atubular glomeruli and the structural basis for chronic renal failure. *Laboratory Investigation* **66**, 265–284.

MARCUSSEN N, OLSEN TS (1989) Atubular glomeruli in patients with chronic pyelonephritis. *Laboratory Investigation* **62**, 467–473.

MARCUSSEN N, JACOBSEN NO (1992) The progression of cisplatin-induced tubulointerstitial nephropathy in rats. *Acta Pathologica et Microbiologica Scandinavica* **100**, 256–268.

MATTFELDT T, MALL G, GHAREHBAGHI H, MOLLER P (1990) Estimation of surface area and length with the orientator. *Journal of Microscopy* **159**, 301–317.

MAYHEW TM (1985) The problem of ambiguous profiles of microvilli between apposed cell surfaces: a stereological solution. *Journal of Microscopy* **139**, 327–330.

MAYHEW TM (1988) An efficient scheme for estimating fibre number from nerve cross-sections: the fractionator. *Journal of Anatomy* **157**, 127–134.

MAYHEW TM (1991*a*) The new stereological methods for interpreting functional morphology from slices of cells and organs. *Experimental Physiology* **76**, 639–665.

MAYHEW TM (1991*b*) The accurate prediction of Purkinje cell number from cerebellar weight can be achieved with the fractionator. *Journal of Comparative Neurology* **308**, 162–168.

MAYHEW TM (1992) A review of recent advances in stereology for quantifying neural structure. *Journal of Neurocytology* **21**, 313–328.

MAYHEW TM, BURGESS AJ, GREGORY CD, ATKINSON ME (1979) On the problem of counting and sizing mitochondria: a general reappraisal based on ultrastructural studies of mammalian lymphocytes. *Cell and Tissue Research* **204**, 297–303.

MAYHEW TM, MACLAREN R, HENERY CC (1990) Fractionator studies on Purkinje cells in the human cerebellum: numbers in right and left halves of male and female brains. *Journal of Anatomy* **169**, 63–70.

MAYHEW TM, MWAMENGELE GLM, SELF TJ, TRAVERS JP (1994*a*) Stereological studies on red corpuscle size produce values different from those obtained using haematocrit- and model-based methods. *British Journal of Haematology* **86**, 355–360.

MAYHEW TM, SIMPSON RA (1994) Quantitative evidence for the spatial dispersal of trophoblast nuclei in human placental villi during gestation. *Placenta* **15**, 837–844.

MAYHEW TM, WADROP E, SIMPSON RA (1994*b*) Proliferative versus hypertrophic growth in tissue subcompartments of human placental villi during gestation. *Journal of Anatomy* **184**, 535–543.

MCMILLAN A-M, SØRENSEN FB (1992) The efficient and unbiased estimation of nuclear size variability using the 'selector'. *Journal of Microscopy* **165**, 433–437.

MENDIS-HANDAGAMA SMLC (1992) Estimation error of Leydig cell numbers in atrophied rat testes due to the assumption of spherical nuclei. *Journal of Microscopy* **168**, 25–32.

MILES RE (1978) The sampling, by quadrats, of planar aggregates. *Journal of Microscopy* **113**, 257–267.

MØLLER A (1992) Mean volume of pigmented neurons in substantia nigra. *Acta Neurologica Scandinavica* **85**, 37–39.

MØLLER A, STRANGE P, GUNDERSEN HJG (1990) Efficient estimation of cell volume and number using the nucleator and disector. *Journal of Microscopy* **159**, 61–71.

MULVANY MJ, BAANDRUP U, GUNDERSEN HJG (1985) Evidence for hyperplasia in mesenteric resistance vessels of spontaneously hypertensive rats using a three-dimensional disector. *Circulation Research* **57**, 794–800.

MWAMENGELE GLM, MAYHEW TM, DANTZER V (1993) Purkinje cell complements in mammalian cerebella and the biases incurred by counting nucleoli. *Journal of Anatomy* **183**, 155–160.

NAIRN JG, BEDI KS, MAYHEW TM, CAMPBELL LF (1989) On the number of Purkinje cells in the human cerebellum: unbiased estimates obtained by using the 'fractionator'. *Journal of Comparative Neurology* **290**, 527–532.

NURCOMBE V, WREFORD NG, BERTRAM JF (1991) The use of the optical disector to estimate the total number of neurons in the developing chick lateral motor column: effects of purified growth factors. *Anatomical Record* **231**, 416–424.

NYENGAARD JR (1993*a*) The quantitative development of glomerular capillaries in rats with special reference to unbiased stereological estimates of their number and sizes. *Microvascular Research* **45**, 243–261.

NYENGAARD JR (1993*b*) Number and dimensions of rat glomerular capillaries in normal development and after nephrectomy. *Kidney International* **43**, 1049–1057.

NYENGAARD JR, BENDTSEN TF, GUNDERSEN HJG (1988) Stereological estimation of the number of capillaries, exemplified by renal glomeruli. *Acta Pathologica et Microbiologica Scandinavica* (suppl. 4), 92–99.

NYENGAARD JR, BENDTSEN TF (1992) Glomerular number and size in relation to age, kidney weight and body surface in normal man. *Anatomical Record* **232**, 194–201.

NYENGAARD JR, GUNDERSEN HJG (1992) The isector: a simple and direct method for generating isotropic, uniform random sections from small specimens. *Journal of Microscopy* **165**, 427–431.

NYENGAARD JR, FLYVBJERG A, RASCH R (1993) The impact of renal growth, regression and repeated growth in experimental diabetes on numbers and sizes of proximal and distal tubular cells in rat kidneys. *Diabetologia* **36**, 1126–1131.

NYENGAARD JR, MARCUSSEN N (1993) The number of glomerular capillaries estimated by an unbiased and efficient stereological method. *Journal of Microscopy* **171**, 27–37.

NYENGAARD JR, RASCH R (1993) The impact of experimental diabetes in rats on glomerular capillary number and sizes. *Diabetologia* **36**, 189–194.

OGBUIHI S, CRUZ-ORIVE L-M (1990) Estimating the total number of lymphatic valves in infant lungs with the fractionator. *Journal of Microscopy* **158**, 19–30.

PAKKENBERG B (1990) Pronounced reduction of total neuron number in mediodorsal thalamic nucleus and nucleus accumbens in schizophrenics. *Archives of General Psychiatry* **47**, 1023–1028.

PAKKENBERG B, GUNDERSEN HJG (1988) Total number of neurons and glial cells in human brain nuclei estimated by the disector and the fractionator. *Journal of Microscopy* **150**, 1–20.

PAKKENBERG B, EVANS SM, MØLLER A, BRAENDGAARD H, GUNDERSEN HJG (1989) Total number of neurons in human neocortex related to age and sex estimated by way of optical disectors. *Acta Stereologica* **8**, 251–256.

PAKKENBERG B, GUNDERSEN HJG (1989) New stereological methods for obtaining unbiased and efficient estimates of total nerve cell number in human brain areas. Exemplified by the mediodorsal thalamic nucleus in schizophrenics. *Acta Pathologica et Microbiologica Scandinavica* **97**, 677–681.

PAKKENBERG B, MØLLER A, GUNDERSEN HJG, MOURITZEN DAM A, PAKKENBERG H (1991) The absolute number of nerve cells in substantia nigra in normal subjects and in patients with Parkinson's disease estimated with an unbiased stereological method. *Journal of Neurology, Neurosurgery, and Psychiatry* **54**, 30–33.

REGEUR L, BADSBERG JENSEN G, PAKKENBERG H, EVANS SM, PAKKENBERG B (1994) No global neocortical nerve cell loss in brains from patients with senile dementia of Alzheimer's type. *Neurobiology of Aging* **15**, 347–352.

SCHMITZ A, NYENGAARD JR, BENDTSEN TF (1990) Glomerular volume in type 2 (non-insulin-dependent) diabetes estimated by a direct and unbiased stereologic method. *Laboratory Investigation* **62**, 108–113.

SIKLOS L, PARDUCZ A, HALASZ N, RICKMANN M, JOO F, WOLFF JR (1990) An unbiased estimation of the total number of synapses in the superior cervical ganglion of adult rats established by the disector method. Lack of change after long-lasting sodium bromide administration. *Journal of Neurocytology* **19**, 443–454.

SIMPSON RA, MAYHEW TM, BARNES PR (1992) From 13 weeks to term, the trophoblast of human placenta grows by the continuous recruitment of new proliferative units: a study of nuclear number using the disector. *Placenta* **13**, 501–512.

SMYTHE E, PYPAERT M, LUCOCQ J, WARREN G (1989) Formation of coated vesicles from coated pits in broken A431 cells. *Journal of Cell Biology* **108**, 843–853.

SØRENSEN FB (1991) Stereological estimation of the mean and variance of nuclear volume from vertical sections. *Journal of Microscopy* **162**, 203–229.

STERIO DC (1984) The unbiased estimation of number and sizes of arbitrary particles using the disector. *Journal of Microscopy* **134**, 127–136.

STRANGE P, MØLLER A, LADEFOGED O, LAM HR, LARSEN JJ, ARLIEN-SOBORG P (1991) Total number and mean cell volume of neocortical neurons in rats exposed to 2,5-hexanedione and 2,5-hexanedione plus acetone. *Neurotoxicological Teratology* **13**, 401–406.

TANDRUP T (1993) A method for unbiased and efficient estimation of number and mean volume of specified neuron subtypes in rat dorsal root ganglion. *Journal of Comparative Neurology* **329**, 269–279.

TANDRUP T, BRAENDGAARD H (1992) The number and mean volume of neurons in the cerebral cortex of rats intoxicated with acrylamide. *Neuropathology and Applied Neurobiology* **18**, 250–258.

TANDRUP T, BRAENDGAARD H (1994) Number and volume of rat dorsal root ganglion cells in acrylamide intoxication. *Journal of Neurocytology* **23**, 242–248.

VEDEL JENSEN EB, GUNDERSEN HJG (1993) The rotator. *Journal of Microscopy* **170**, 35–44.

WEIBEL ER (1979) *Stereological Methods*, vol. 1, *Practical Methods for Biological Morphometry*. London: Academic Press.

WERNERSON A, SVENSSON O, REINHOLT FP (1989) Parathyroid cell number and size in hypercalcemic rats: a stereologic study employing modern unbiased estimators. *Journal of Bone and Mineral Research* **4**, 705–713.

WEST MJ (1993*a*) New stereological methods for counting neurons. *Neurobiology of Aging* **14**, 275–285.

WEST MJ (1993*b*) Regionally specific loss of neurons in the aging human hippocampus. *Neurobiology of Aging* **14**, 287–293.

WEST MJ, COLEMAN PD, FLOOD DG (1988) Estimating the number of granule cells in the dentate gyrus with the disector. *Brain Research* **448**, 167–172.

WEST MJ, GUNDERSEN HJG (1990) Unbiased stereological estimation of the number of neurons in the human hippocampus. *Journal of Comparative Neurology* **296**, 1–22.

WEST MJ, SLOMIANKA L, GUNDERSEN HJG (1991) Unbiased stereological estimation of the total number of neurons in the subdivisions of the rat hippocampus using the optical fractionator. *Anatomical Record* **231**, 482–497.

WIGMORE PM, BAILLIE HS, KHAN M, MORRISON EH, MAYHEW TM (1992) Nuclear number during muscle development. *Muscle and Nerve* **15**, 1301–1302.

YOUNGS TA, BOYCE RW, MOSEKILDE L, SØGAARD CH, PADDOCK CL, GUNDERSEN HJG (1994) Direct stereological estimation of 3D connectivity density in human iliac cancellous bone: the effect of age and sex. *Acta Stereologica* **13**, 55–60.

ZHAO HQ, MACDONALD IF (1993) An unbiased and efficient procedure for 3-D connectivity measurement as applied to porous media. *Journal of Microscopy* **172**, 157–162.